Importance of Many-Body Effects in the Clustering of Charged Zn Dopant Atoms in GaAs

Ph. Ebert,[1] Tianjiao Zhang,[2,3] F. Kluge,[1] M. Simon,[1] Zhenyu Zhang,[3,2] and K. Urban[1]
[1]*Institut für Festkörperforschung, Forschungszentrum Jülich GmbH, 52425 Jülich, Germany*
[2]*Department of Physics, University of Tennessee, Knoxville, Tennessee 37996*
[3]*Solid State Division, Oak Ridge National Laboratory, Oak Ridge, Tennessee 37831-6032*
(Received 10 May 1999)

The spatial distribution of negatively charged Zn dopant atoms in GaAs has been investigated by cross-sectional scanning tunneling microscopy. At high densities, the dopant atoms exhibit clear clustering behavior, suggesting the existence of an effective attractive interaction in addition to the screened Coulomb repulsion between two dopants. By analyzing the data through Monte Carlo simulations, we have extracted the intrinsic screening length at different dopant densities and attributed the origin of the effective attraction to strong many-body effects in the dopant-dopant repulsion.

PACS numbers: 61.72.Ss, 61.16.Ch, 81.05.Ea, 85.40.Ry

The ability to incorporate reproducibly dopant atoms with precisely controlled concentrations and spatial distributions is essential in various technological applications of semiconductor materials. As the effort for device miniaturization continues to intensify, to achieve this goal is becoming increasingly difficult. Dopant incorporation in submicrometer- and nanometer-scale systems is ultimately governed by the intrinsic interactions between the dopant atoms. The generally accepted view is that the charge of a dopant atom is screened by the charge carriers in a given semiconductor, resulting in a repulsive screened Coulomb interaction between the dopants [1]. Such a repulsion in turn will lead to a rather homogeneous distribution of the dopant atoms in the semiconductor.

In this Letter, we use cross-sectional scanning tunneling microscopy (XSTM) to demonstrate that negatively charged Zn dopant atoms in GaAs are inhomogeneously distributed and form clusters of dopant atoms. At first sight, the clustering behavior seems to suggest the existence of a possible attractive interaction in addition to the screened Coulomb repulsion between the dopants. But our quantitative analysis of the dopant distributions by Monte Carlo simulations convincingly shows that the effective attraction actually results from strong many-body effects in the repulsive dopant-dopant interactions. We also illustrate the methodology to determine quantitatively the intrinsic screening length of point charges in the semiconductor based on XSTM images.

We investigated Zn-doped GaAs crystals with different carrier concentrations (n) ranging between 2.5×10^{18} and 2.5×10^{20} cm^{-3}. The Zn dopant atoms were introduced into the crystals during growth ($n < 10^{20}$ cm^{-3}) or by Zn diffusion at $\approx$1180 K ($n > 10^{20}$ cm^{-3}). The crystals were slowly cooled down to room temperature after growth with the exception of Zn-diffused crystals, which were quenched to room temperature. Thus the dopant atoms reached an equilibrium at a freeze-in temperature of GaAs or in the case of Zn-diffused material at $\approx$1180 K. Samples cut from the different crystals were cleaved in ultrahigh vacuum (5×10^{-9} Pa) and the isolated dopant atoms exposed on the (110) cleavage surfaces were imaged with atomic resolution by XSTM.

Figure 1(a) shows a typical STM image of such a cleavage surface of a GaAs crystal doped with 2.5×10^{20}Zn cm^{-3}. The image shows the occupied density of states above the As atoms acquired at negative sample voltage [2]. The atomic-scale corrugation arising from the atomic rows along the $[1\bar{1}0]$ direction can be recognized as rows from the upper right to the lower left corner. Localized bright contrast features arise from isolated dopant atoms [3]. The few localized dark contrasts are due to vacancies formed mostly after cleavage [4]. The localized contrast of the dopant atoms and vacancies arises from the imaging of the local screening potential around the isolated defects or dopants [5].

One of the most distinctive features in the STM images is the long-range contrast change (on the scale of about 5 to 10 nm) superposed on the localized features of the dopant atoms. The long-range contrast becomes more pronounced at lower magnitudes of the voltage, indicating that it is the signature of variations of the local band bending, namely, the position of the valence band edge changes locally relative to the Fermi level [5]. In order to unravel the origin of this effect, we deduced from Fig. 1(a) the positions of all the dopant atoms based on their local contrast discussed in Ref. [3] [Fig. 1(b)] and calculated the local concentrations [Fig. 1(c)]. High concentration of dopant atoms is displayed as white areas; in contrast, the local concentration of dopants is a factor of 8 lower in the dark areas. Figure 1(c) demonstrates that the concentration of the dopant atoms varies by nearly 1 order of magnitude on the scale of about 10 nm and all the bright areas in Fig. 1(c) correspond to the bright areas in Fig. 1(a). Thus local fluctuations of the dopant concentration on the scale of about 10 nm by nearly 1 order of magnitude cause fluctuations of the Fermi level on the same scale imaged as long-range contrast in Fig. 1(a). Figure 1 also demonstrates that the dopant atoms tend to cluster. We have observed a clustering of dopants in all the samples investigated, including those

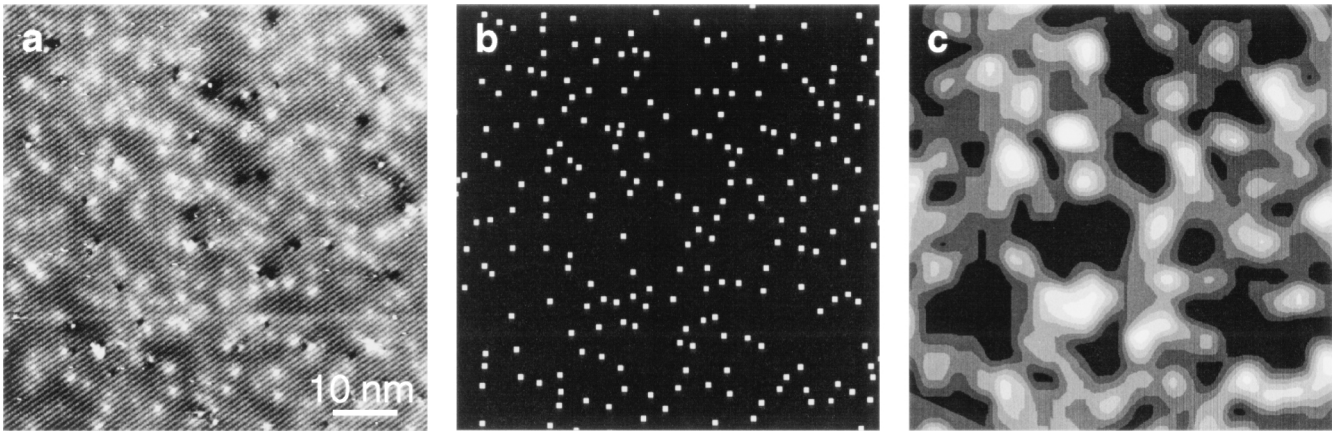

FIG. 1. (a) STM image of a (110) cleavage surface of Zn-doped GaAs acquired at −2.4 V. A long-range contrast variation is superposed onto the atomic-scale corrugation of the atomic rows along the $[1\bar{1}0]$ direction. The bright and dark contrast features are dopant atoms and vacancies, respectively. (b) Positions of the dopant atoms in (a). (c) Local concentration of the dopant atoms. A high concentration is shown as white contrast. The images show a clustering of the dopant atoms.

grown by different methods, doped by diffusion and during crystal growth, and in different materials (GaAs and InP). Thus the observed effect is not simply due to sample preparation, but rather an intrinsic nature of the dopants. To our knowledge this is the first direct observation of clustering of dopant atoms on such a length scale.

As mentioned earlier, all the dopant atoms are negatively charged and should therefore mutually interact with the repulsive screened Coulomb potential. Nevertheless, the clustering behavior suggests the possible existence of a long-range attractive interaction between the dopants. In trying to identify the physical origin of the attraction, several candidates may come to mind, such as stress effects associated with the dopants [6], attractive forces caused by the oscillatory nature of the screening charge surrounding each dopant, or just a statistical distribution. In the following, we will show that, rather than any of those possibilities, the effective attraction is most simply accounted for by considering the many-body (or correlation) effects in the otherwise strictly repulsive screened Coulomb interaction. As described below, consideration of the correlation effects also naturally resolves another puzzle related to the apparent screening length of the repulsive potential in the semiconductor.

We proceed by first studying the effects of the short-range repulsion on the dopant distribution. The existence of the short-range repulsion is clearly indicated by the fact that although clustering occurs the probability of finding a very close pair of dopant atoms is negligible. In order to quantify the repulsive interaction we deduced from the XSTM images the positions of all the dopant atoms and calculated the distances r between all possible pairs of dopants [7–9]. This gives us the measured probability distribution of pair distances. Dividing the measured probability distribution of pair distances by the one for noninteraction, randomly distributed dopant atoms results in the pair correlation function $c(r)$, which is related to the mean force potential, $W(r)$, through [10]

$$W(r) = -kT \cdot \ln[c(r)]. \tag{1}$$

It should be noted that only if the extension of the interaction is smaller than the average separation of the dopants, correlation effects can be neglected and the mean force potential equals the interaction energy.

Figure 2(a) shows the values $-\ln[c(r)]$ for three carrier concentrations as a function of the distance r. First, we observed in all cases a repulsive interaction, whose extension increases from 2 to 5 nm if the carrier concentration decreases from 2.5×10^{20} to 2.5×10^{18} cm^{-3}. This reflects the repulsive screened Coulomb interaction between two equal charges and the carrier concentration dependence of the screening. It is well known that the charge of a dopant atom in a semiconductor is screened by the charge carriers, leading to a screened Coulomb potential surrounding each dopant [1]

$$V(r) = \frac{e}{4\pi\varepsilon_0\varepsilon_r} \cdot \frac{1}{r} \cdot e^{-\frac{r}{R_S}}, \tag{2}$$

with R_S being the screening length

$$R_S = \sqrt{\frac{2\pi^2\varepsilon_0\varepsilon_r\hbar^3}{e^2(m_e)^{3/2} \cdot (2\pi kT)^{1/2} \cdot F_{-1/2}\{\eta\}}}. \tag{3}$$

$F_k\{\eta\}$ are the Fermi-Dirac integrals with the reduced Fermi energy $\eta = E_F/kT$.

If we assume the low dopant density limit, we can fit the data shown in Fig. 2(a) with a Yukawa potential and determine the screening length as a function of the carrier concentration [filled squares in Fig. 2(b)]. As expected, the screening length increases with decreasing carrier concentration. However, the data do not agree quantitatively with the theoretical values for the screening length [solid line in Fig. 2(b)] determined according to Eq. (3) for a freeze-in temperature of 900 K.

The effective attraction between the dopants and the substantial discrepancy in the screening lengths described

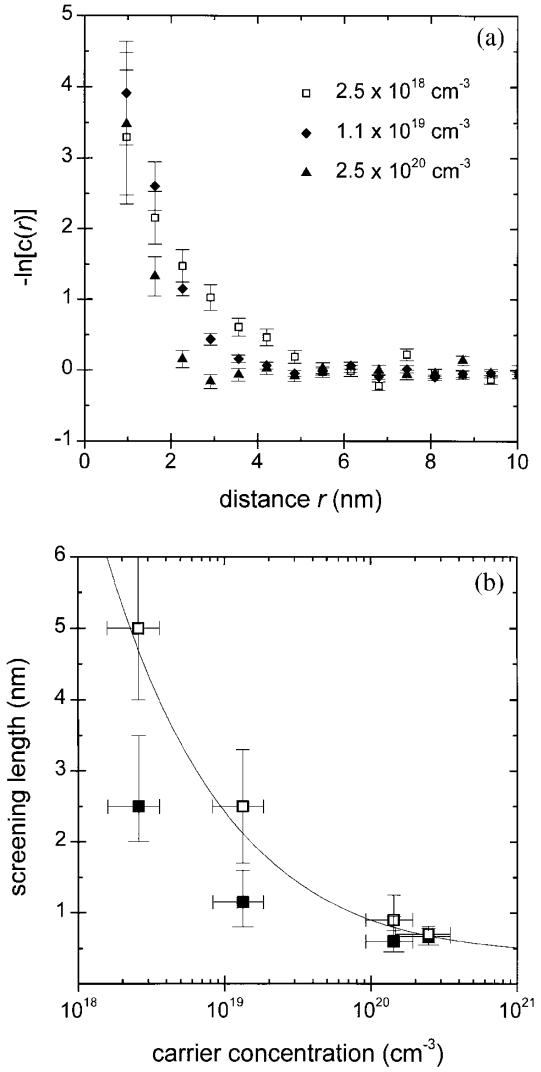

FIG. 2. (a) Negative logarithm of the pair correlation function for three carrier concentrations and (b) values for screening lengths R_S determined in (a) as a function of the carrier concentration (filled squares). The solid line represents the theoretical screening length calculated according to Eq. (3). The open squares show the screening length corrected for many-body interactions.

above both strongly suggest the importance of many-body effects in the otherwise repulsive interaction between the dopants. As known previously, for a collection of mutually repelling particles, strong many-body effects can result in oscillatory features in the pair correlation function, with the minima indicating effective attractive interactions [7,10]. Furthermore, if the repulsion is a screened one such as that described by Eq. (2), many-body effects can also result in a shorter apparent screening length than the true one. To demonstrate that this is indeed the case for the present system, we have performed Monte Carlo simulations of the experiment. In the simulations, we positioned randomly 8000 dopant atoms surrounded by a screened Coulomb potential in a three-dimensional model crystal and allowed them to migrate to reach an equilibrium configuration. We took the boundary effects into account. In a real crystal the dopant atoms have to overcome some migration barrier in order to change their lattice position. It is rather difficult to implement this in our calculation, because the exact diffusion mechanism of Zn dopant atoms in GaAs is very complex. It is usually assumed that the dopant atoms diffuse in interstitial sites rather fast until they retake a substitutional lattice site by kicking out the Ga atom on that site [11]. This process occurs at elevated temperature and freezes in during the slow cooling process of the crystal growth procedure. From the data about Zn diffusion [11] we estimate the freeze-in temperature to be about 900 K. It is reasonable to assume that the effect of Coulomb interactions is felt by the dopants independent of the details of the migration path, because the energy of a specific lattice site is affected by the electrostatic screened Coulomb potential induced by neighboring dopants. This consideration allows us to simulate the effect of the pair screened Coulomb interactions on the final spatial configuration of the dopant atoms without specifying the exact diffusion path. Specifically, we assume that the dopant interaction leads to an additional potential added to the trapping potential at a substitutional site. Therefore we allowed the dopant atoms to migrate with an energy equivalent to a temperature of about 50 K only within the screened Coulomb pair interaction potentials. In the real crystal this simulates the case where the diffusion occurs at freeze-in temperature plus 50 K. Simulations with different temperatures showed that within a reasonable temperature range the exact choice of the temperature does not change the results significantly.

After reaching the equilibrium configuration we analyzed the spatial distribution as we did for the XSTM images. We determined the (output) screening length from the simulated pair correlation function for different (input) screening lengths of the Yukawa potential. The results show that for very low dopant concentrations the input and output screening lengths are equal. At the experimental dopant concentrations the output screening lengths are considerably smaller than the input screening lengths due to many-body effects, i.e., interactions between more than two dopant atoms. Using these simulations we determined the intrinsic screening length in the GaAs crystals as a function of the carrier concentration by comparing the measured screening length with the output screening length of the simulation. The corresponding input screening length is the intrinsic one. The input screening lengths [empty squares in Fig. 2(b)] agree very well with the theoretical calculations according to Eq. (3) at 900 K (solid line). (The data obtained on Zn-diffused GaAs at 1180 K agree too, because at $n > 10^{20}$ cm^{-3} the screening length is only very weakly dependent on the temperature.) The error bars of the corrected values arise from the error bars of the measurement and the error estimation of the simulation. We note that Fig. 2(b) shows the

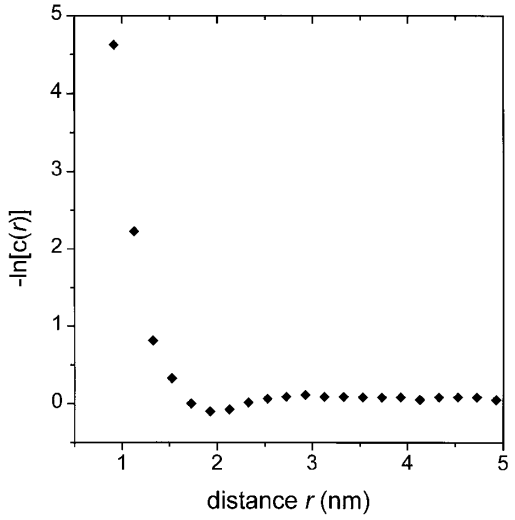

FIG. 3. Simulated negative logarithm of the pair correlation function with many-body interactions for a dopant concentration of 1.5×10^{20} cm^{-3}.

first quantitative microscopic measurement of the screening length in semiconductors.

The good agreement in the screening length with consideration of many-body effects and that from the classical screening theory indicates that the present system can be well described by the classical screening. The importance of many-body effects is further corroborated by the simulated pair correlation function in Fig. 3, which shows a clear attractive part beyond a short-range repulsive core. We note that an attractive part becomes most pronounced in the experimentally determined pair correlation function for the highest doped sample. The effective attractive interaction potential is the result of many-body effects [10] and leads to the clustering of dopant atoms observed experimentally. This conclusion is consistent with the observation that clustering of dopant atoms occurs independent of the semiconductor material, growth conditions, dopant element, and the technique of dopant incorporation. The model used is based only on the presence of charges in a material with a limited carrier concentration. At this stage we discuss other possible sources of attractive dopant interactions. Stress-related forces induced by substitional Zn atoms can be excluded, because Zn atoms have nearly the same covalent radius as Ga atoms, which they substitute. Friedel oscillations can also be ruled out, because they should be too weak in strength at the elevated temperatures, and we found no indication of them in STM images. Van der Waals forces induced by fluctuations of the screening cloud can result in attractions, which are, however, also too weak compared to the direct Coulomb interactions. The simulations and the measured data allowed also to exclude statistical variations of dopant concentrations with no many-body interactions to be the origin of the clustering. Thus there are so far only many-body effects of the screened Coulomb interactions of dopant atoms, which are consistent with the experimental data.

In conclusion, we have used cross-sectional scanning tunneling microscopy to demonstrate that negatively charged Zn dopant atoms in GaAs are inhomogeneously distributed and form clusters of dopant atoms. The clustering behavior suggests the existence of a possible attractive interaction in addition to the screened Coulomb repulsion between the dopants. Our quantitative analysis of the dopant distributions by Monte Carlo simulations leads to the conclusion that the effective attraction actually results from strong many-body effects in the otherwise repulsive dopant-dopant interactions. Many-body effects are also shown to be important in extracting the intrinsic screening length of the Yukawa potential as a function of the carrier concentration in the system. Our study reveals a basic physical origin limiting the homogeneity of dopant atoms achievable in semiconductors.

We thank S. Pantelides, K. Horn, and K. Schroeder for helpful discussions, K. H. Graf for technical support, and D. Henkel for software support. This work was supported in part by the ORNL managed by Lockheed Martin Energy Research Corp. for the U.S. Department of Energy under Contract No. DEAC05-96OR22464, by the NSF under Grant No. DMR-9705406, and by the University of Tennessee.

[1] R. B. Dingle, Philos. Mag. **46**, 861 (1955).
[2] R. M. Feenstra *et al.*, Phys. Rev. Lett. **58**, 1192 (1987); Ph. Ebert *et al.*, Phys. Rev. Lett. **77**, 2997 (1996).
[3] M. B. Johnson *et al.*, Appl. Phys. Lett. **63**, 2923 (1993).
[4] Ph. Ebert *et al.*, Phys. Rev. B **51**, 9696 (1995); Ph. Ebert, K. Urban, and M. G. Lagally, Phys. Rev. Lett. **72**, 840 (1994); G. Lengel *et al.*, Phys. Rev. Lett. **72**, 836 (1994).
[5] J. A. Stroscio, R. M. Feenstra, and A. P. Fein, Phys. Rev. Lett. **58**, 1668 (1987); R. J. Hamers, J. Vac. Sci. Technol. B **6**, 1462 (1988); C. Domke *et al.*, J. Vac. Sci. Technol. B **16**, 2825 (1998).
[6] J. B. Mullin *et al.*, J. Appl. Phys. **47**, 2584 (1976).
[7] T. T. Tsong, Phys. Rev. Lett. **31**, 1207 (1973).
[8] Ph. Ebert *et al.*, Phys. Rev. Lett. **76**, 2089 (1996).
[9] K.-J. Chao *et al.*, Phys. Rev. Lett. **79**, 4822 (1997).
[10] T. L. Hill, *Statistical Mechanics* (McGraw-Hill, New York, 1956).
[11] S. Yu, T. Y. Tan, and U. Gösele, J. Appl. Phys. **69**, 3547 (1991).